Journal of Nuclear Materials 438 (2013) S861–S864

Contents lists available at SciVerse ScienceDirect

Journal of Nuclear Materials

journal homepage: www.elsevier.com/locate/jnucmat

On "bubbly" structures in plasma facing components

S.I. Krasheninnikov *[,1], R.D. Smirnov

University of California at San Diego, La Jolla, CA 92093, USA

ARTICLE INFO

Article history:
Available online 17 January 2013

ABSTRACT

The theoretical model of "fuzz" growth describing the main features observed in experiments is discussed. This model is based on the assumption of enhancement of plasticity of tungsten containing significant fraction of helium atoms and clusters. The results of molecular dynamics (MD) simulations support this idea and demonstrate strong reduction of the yield strength for all temperature range. The MD simulations also show that the "flow" of tungsten strongly facilitates coagulation of helium clusters, which otherwise practically immobile, and the formation of nano-bubbles.

1. Introduction

It was known for a long time that the presence of hydrogen and helium in the solids could result in the formation of bubbles and blisters. For the case of fusion devices hydrogen and helium can appear in the metals due to irradiation of the first wall with hydrogen/helium plasma and neutron irradiation of material structures in burning plasma devices, which causes helium accumulation associated with neutron induced nuclear reactions [1].

Recent more detailed experiments on tungsten irradiation with low energy (below 100 eV) hydrogen/helium plasma, relevant to the near-wall plasma conditions in magnetic fusion reactor like ITER, demonstrated a very dramatic change in both surface morphology and near surface material structure of the samples. In particular, it appears that for some conditions a long (mm-scale) and thin (nm-scale) fiber-like structures filled with nano-bubbles, so-called "fuzz", start to grow [2–5].

According to the experimental data from Ref. [3], the dynamics of the "fuzz" growth is sensitive to the sample temperature, T, and also depends on the flux of helium ions, Γ_{He}. However, for helium flux exceeding $\sim 10^{22}$ m^{-2} s^{-1} the dependence on Γ_{He} vanishes and the thickness of the "fuzz", L_{fuzz}, scales with plasma irradiation time, t_{irrad}, as $L_{fuzz} \propto \sqrt{t_{irrad}} \exp(-E_{fuzz}/T)$ with $E_{fuzz} \sim 0.35$eV.

Although the "fuzz" growth only within a certain range of sample temperature (1000 K < T < 2000 K) and the energy of impinging helium ions (above ~20 eV) [4,5], outside this region other types of a strong material modification also occurs under hydrogen/helium plasma irradiation. For example, for T above 2000 K a large ~mm rough pinhole-structures start to develop, while for the projectile energy below 20 eV the holes appear at rather smooth surface, for T below 1000 K the surface becomes rather rough and under the surface a large amount of nano-bubbles is formed.

According to experimental data from [6] "fuzz" is growing virtually on any kind of tungsten, the results of Ref. [7] show the sensitivity of "fuzz" growth on particular type of tungsten. In addition to that, impurities (beryllium and carbon) can prevent "fuzz" growth for the case of low projectile energy where the sputtering of Be and/or C is negligible so that Be and/or C layer can be formed on the tungsten surface [8].

Apart from the surface modification, the formation of bubbles and structures strongly modify other properties of tungsten. For example in Refs. [9,10] it was shown that the hydrogen retention in tungsten is modified under hydrogen/helium plasma irradiation. It increases at high (~1600 K) and reduces at low (~700 K) temperatures. In addition, the "fuzzy" structure of the surface can trigger arcs [11].

At large energy of impinging helium ions (in the range of tens of keV) a strong modification of tungsten surface (e.g. formation of a large craters, which probably related to large bubble formation [12,13]) was also observed [14–16].

We notice that the formation of "fuzz" on tungsten is not unique, and as a matter of fact it was also observed on molybdenum under irradiation by low energy helium plasma [17] and on the rhodium under hydrogen plasma irradiation [18]. Thus, it seems that "fuzz" is very generic and, therefore, suppose to exhibit some fundamental properties of solid material filled with the gas bubbles.

In harsh tokamak environment "fuzz" might not survive due to high heat loads to the surface during, for example, transient events (e.g. ELMs and disruptions). Indeed, even transient overheating of the surface above temperature ~2000 K, where "fuzz" disappears, would prevent continuous accumulation of "fuzz". The impact of such effect is supported by experiments on linear devices with transient heating of the sample by the laser pulses [19,20]. An exposure of the preformed "fuzz" to the TEXTOR tokamak plasma

* Corresponding author. Address: UCSD, 9500 Gilman Dr., La Jolla, CA 9209-0411, USA.
E-mail address: skrash@mae.ucsd.edu (S.I. Krasheninnikov).
[1] Presenting author.

0022-3115/$ - see front matter © 2013 Elsevier B.V. All rights reserved.
http://dx.doi.org/10.1016/j.jnucmat.2013.01.186

also shows "fuzz" disintegration in a way similar to that on linear devices with laser heat pulses. But in addition to that it was found that "fuzz" is starting to be covered with carbon, which was present in the machine. Nonetheless, recently "fuzz" was observed on tungsten surface in Alcator C-Mod tokamak [21].

Thus we see that the formation of "bubbly" structures, including "fuzz", plays very important role in evolution of surface morphology. In addition, experimental results with other materials show that here we are dealing with some fundamental issue of the interactions of noble gases with the metals. However, the physical mechanism of the "fuzz" growth is not clear. At this moment there are two different opinions on this point. In Ref. [22] a qualitative picture of the "fuzz" growth was suggested, which is based on the formation of small bubbles the coalescence of which results in bursting of blisters and further formation of the bubbles at the bottom of protrusions. However, this model has difficulties with explanation of how impinging helium can penetrate through thick "fuzzy" layer of tungsten all the way to the bottom of the protrusions. Another model [23] is based on the assumption of enhanced plasticity of tungsten with large concentration of entrained helium atoms and clusters, which can play similar role to that played by lattice defects resulting in well known irradiation creep (e.g. see Ref. [24]). The standard creep theories [25] show that within the temperature range of interest 1000–2000 K an impact of the creep is negligible. However standard creep models assume that the dislocations, which finally cause the creep, appear in the material only due to applied stress. Meanwhile in our case very large stresses and lattice defects always present in tungsten due to the large amount of helium atoms/clusters in tungsten's lattice due to plasma irradiation (e.g. see Ref. [26] and the references therein), which standard theory do not account for.

In Section 2 we review the main assumptions and results of model from Ref. [23]. In Section 3 we present the results of the Molecular Dynamics (MD) simulations supporting the idea of enhanced plasticity of tungsten with large concentration of entrained helium atoms and clusters and also elucidating the role of material plasticity in the cluster coalescence and bubble growth. In Section 4 we summarize our main conclusions.

2. "Visco-elastic" model of "fuzz" growth

The main idea behind the "visco-elastic" model [23] is an assumption that the presence of large amount of helium atoms and clusters in the tungsten lattice can significantly alter tungsten's plasticity. Then tungsten under some applied stresses can move ("flow"). In a simplest version this motion can be described as an incompressible material flow under impact of a stress with effective viscosity $\mu(T) = \bar{\mu}\exp(E_\mu/T)$, where $\bar{\mu}$ is the normalization constant, and E_μ is the activation energy, which can be found by the fitting of experimental data on the "fuzz" growth rate [23]. We notice that at low temperatures effective viscosity becomes very large and, therefore, both tungsten motion and "fuzz" growth virtually do not exist (within this simplified description it may be interpreted as a small elastic deformation).

At relatively high temperature the effective viscosity becomes low enough so that the plastic deformation starts to be important. Due to continuous flux of helium ions newly seeded bubble starts to grow on the top of the old one (see Fig. 1) causing additional stress in tungsten and, correspondingly, the flow of tungsten from the base to the top of a new bubble which finally results in the formation of nano-fiber. In general case the fiber growth depends on both helium and tungsten supplies to the newly growing bubble. However, it is obvious that in practice the slower process determines the fiber growth rate. In Ref. [23] it was assumed that the tungsten supply limits the growth rate.

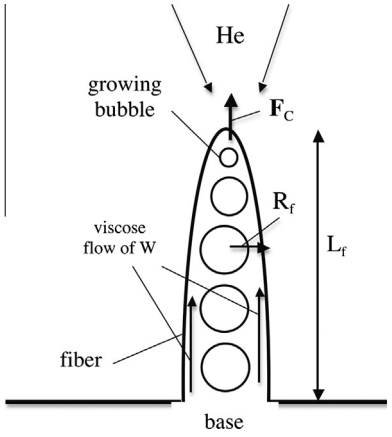

Fig. 1. Schematic views of the fiber growth and "viscose flow" of W to the tip of the fiber due to the force caused by the pressure of the He in the growing fiber.

The estimate of the rate of the fiber growth can be found considering the force balance imposed by the bubble at the very tip of the fiber and the viscose flow of the tungsten in the fiber's "skin". As a result, one finds [23]:

$$L_f(t_{irrad}) = \sqrt{\frac{2\gamma\delta_f}{\mu}t_{irrad}}, \quad (1)$$

where $L_f(t)$ is the length of the fiber, δ_f is the thickness of the fiber "skin", and γ is the tungsten surface tension coefficient.

This tungsten flow limited model of "fuzz" growth is valid for the helium flux to the sample satisfying inequality $\Gamma_{He} \gtrsim n_{He} dL_f/dt$, where $n_{He} \sim 10^{29}$ m^{-3} is the helium particle density in the bubbles. It was estimated (see Ref. [23]) that this inequality is satisfied for $\Gamma_{He} > \Gamma_{He}^{min} \sim 10^{22}$ m^{-2} s^{-1} .

At high temperatures one needs to take into account helium detrapping from the bubbles filling the fibers, which will slow down the eventually prohibit the "fuzz" growth. This effect starts to be important for $T \gtrsim T_h \sim 2000$ K [23].

Thus we see that the assumption of enhanced tungsten plasticity in the presence of large amount of helium atoms and clusters in the tungsten lattice [23] allows to develop the model of "fuzz" growth which reproduces all major experimental observations: $t^{1/2}$ growth of length of the fibers, strong temperature dependence of the growth rate, the saturation of the growth with ion helium flux to the substrate exceeding $\sim 10^{22}$ m^{-2} s^{-1}, and the termination of "fuzz" growth at the temperatures above ~2000 K.

However, till now there were neither experimental nor theoretical results directly supporting the enhanced tungsten plasticity in the presence of large amount of helium atoms and clusters in the tungsten lattice, which might cast some doubts on the applicability of this model.

3. MD simulation of the impact of entrained helium on tungsten plasticity

In this section we present initial results of the MD modeling of the yield strength of nano-sized tungsten material under shear load applied. More complete results can be found in [27]. We employ the MD code LAMMPS [28], allowing to use a wide variety of empirical inter-atomic potential styles that is important for mixed material simulations. In our simulations we use EAM/Finnis–Sinclair type potential for W–W atom interactions produced by Ackland and available at NIST collection of atomic potentials [29], which demonstrates good agreement of simulated ideal shear strength of tungsten with experimental measurements [30]. The

W–He interactions are modeled by ZBL universal repulsive potential [31], which is often used as a fit of *ab initio* inter-atomic potentials at short range. The *ab initio* potential for W–He pair reported in [32] demonstrates a small 9 meV potential minimum at distance ~2.4 Å that is not essential for temperatures of 300–2500 K, for which our simulations were performed. For He–He interactions, we used the *de facto* standard empirical potential proposed by Beck [33]. All potentials were cut-off at the same length of 4.11 Å. Let us note that no empirical potential can reproduce all material properties precisely. Therefore, results reported here should be considered as an approximation that allows qualitative analysis of material properties and demonstrates dependencies of these properties on externally controllable parameters. Such dependencies can serve as a guideline for further experimental investigations of helium-exposed tungsten.

For the described above purposes, we model a slab of monocrystalline BCC tungsten of size of 10 unit cells in each of the three dimensions. Periodic boundary conditions are used in the *X*, *Z* orthogonal directions and free surface conditions are applied in the *Y* direction. Here we present the results for crystal orientation where the free surfaces are {0 1 0} tungsten crystallographic planes. The size of the simulated slab in the *Y* direction is 3.16 nm. A number of helium atoms given by an atomic percentage relative to number of tungsten atoms are initially randomly distributed in the slab volume. To equilibrate the system, its total potential energy first was minimized using conjugate gradient relaxation method and then the sample was annealed at a given temperature for 0.1 ns. During the equilibration process, some helium atoms formed clusters or could leave the material at high initial concentrations of dissolved helium and high system temperatures. The initial random positions of the helium atoms were the same for all simulations. During the simulations the temperature of tungsten and helium atoms was maintained at a given value using Berendsen rescaling technique.

After initial equilibration, the forces were applied to tungsten atoms that belong to the unit cells adjacent to the free boundary surfaces. To produce shear stress in the sample, the forces were applied antiparallel at the two free surfaces along the *X*-axis chosen as ⟨1 0 0⟩ crystallographic direction in {0 1 0} plane. The magnitude of the forces on each affected atom was linearly ramped up from zero to material failure point with rate 1 eV/(Å ns) that corresponds to the applied shear stress increase rate of 16 GPa/ns. An impact of applied shear stress increase rate on both the yield and the applicability of inter-particle potentials will be discussed in Ref. [27]. Taking Young's modulus ~400 GPa as for pure tungsten, we can estimate the order of the produced shear strain rate as $5 \times 10^7\ s^{-1}$. The simulations continued with 1 fs time-step until the material ultimately starts to exhibit plastic deformation.

In Fig. 2 the dependencies of shear yield strength on temperature of the simulated system are plotted for different initial atomic concentrations of dissolved helium. The shear yield strength, τ_Y, was evaluated at the point of apparent skid of the boundary tungsten atoms relative to underlying atomic layers. The simulated strength for pure tungsten at 300 K is found to be in a good agreement with experimental tungsten shear strength [30]. However, as one can see in Fig. 2 the yield strength decreases with increased atomic concentration of the dissolved helium atoms. This can be explained by increase of the potential energy of the system and the associated increase of probability of formation of lattice defects responsible for plastic deformation. The simulations show that the yield strength is generally a decreasing function of temperature, except for the cases of low-to-moderate helium concentrations, where anomalies at temperatures ~900–1200 K can be observed, which, probably, are associated with activation of diffusion and partial loss of helium atoms from the sample (although further studies of this effect are necessary). For n[He] ~ 10 at.% the yield strength shows week temperature dependence, which may be related to inception of helium clusters coagulation to larger bubbles at this concentrations. The simulated yield strength at temperature 1000 K and high helium concentrations >10 at.% is ~5 GPa, which in a ballpark consistent with the pressure created in the helium bubbles.

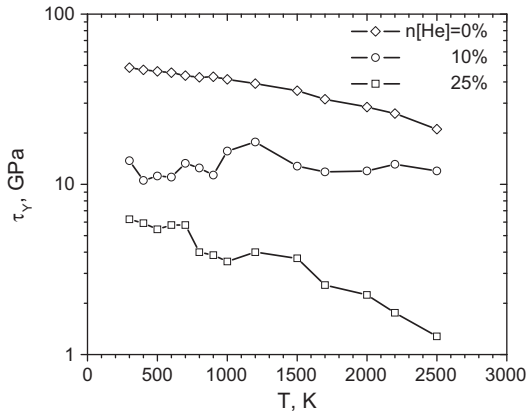

Fig. 2. Simulated dependencies of the shear yield strength of tungsten with different initial atomic concentrations of dissolved helium for shear stress applied in {0 1 0}⟨1 0 0⟩ direction.

Thus the preliminary results of MD simulation support the idea of enhancement of plasticity of tungsten containing significant fraction of helium atoms and clusters. However, more work is needed to quantify both the magnitude of effective viscosity corresponding to plastic deformation and its temperature dependence (in particular, the high strain rates, used in our simulations, could affect the results). We also found from MD simulations that the "flow" of tungsten strongly facilitates coagulation of helium clusters (otherwise practically immobile) and the formation of nano-bubbles [27].

4. Conclusions

We outline the main features of so-called "visco-elastic" "fuzz" growth [23], which is based on the assumption of enhancement of plasticity of tungsten containing significant fraction of helium atoms and clusters. The results of the MD simulations, presented here, support this idea and demonstrate strong reduction of the yield strength for all temperature range. The MD simulations also show that the "flow" of tungsten strongly facilitates coagulation of helium clusters, which otherwise practically immobile, and the formation of nano-bubbles. In order to have complete self-consistent picture of "fuzz" growth, further effort is needed to build up a computational model, which would incorporates: MD simulation results on tungsten plasticity in the presence of dissolved helium, formation of helium bubbles, stresses in material, and the motion of the tungsten.

Acknowledgments

We acknowledge discussions of the proper choice of inter-atomic potentials with N. Juslin and A.V. Krasheninnikov. Work was performed under the auspices of USDOE Grant No. DE-FG02-04ER54739 and the PSI Science Center Grant DE-SC0001999 at UCSD.

References

[1] M.I. Guseva, Yu.V. Martynenko, Sov. Phys. Uspekhi 24 (1981) 996.
[2] S. Takamura, N. Ohno, D. Nishijima, S. Kajita, Plasma Fusion Res. 1 (2006) 051.

[3] M.J. Baldwin, R.P. Doerner, Nucl. Fusion 48 (2008) 035001.
[4] S. Kajita et al., Nucl. Fusion 49 (2009) 095005.
[5] M.J. Baldwin, T.C. Lynch, R.P. Doerner, J.H. Yu, J. Nucl. Mater. 415 (2011) S104.
[6] M.J. Baldwin, R.P. Doerner, J. Nucl. Mater. 404 (2010) 165.
[7] M. Yamagiwa et al., J. Nucl. Mater. 417 (2011) 499.
[8] M.J. Baldwin et al., J. Nucl. Mater. 390–391 (2009) 885.
[9] D. Nishijima et al., J. Nucl. Mater. 337–339 (2005) 927.
[10] M. Miyamoto et al., J. Nucl. Mater. 415 (2011) S657.
[11] S. Kajita, N. Ohno, S. Takamura, Nucl. Fusion 49 (2009) 032002.
[12] S. Sharafat et al., J. Nucl. Mater. 386–388 (2009) 900.
[13] S. Sharafat et al., J. Nucl. Mater. 389 (2009) 203.
[14] B.B. Cipiti, G.L. Kulcinski, J. Nucl. Mater. 347 (2005) 298.
[15] R.F. Radel, G.L. Kulcinski, J. Nucl. Mater. 367–370 (2007) 434.
[16] M. Tokitani et al., Plasma Fusion Res. 5 (2010) 012.
[17] S. Kajita et al., J. Nucl. Mater. 417 (2011) 838.
[18] R.P. Doerner, private communication, 2011.
[19] S. Kajita et al., Nucl. Fusion 47 (2007) 1358.
[20] S. Kajita, N. Ohno, W. Sakaguchi, M. Takagi, Plasma Fusion Res. 4 (2009) 004.
[21] D. White, private communication, 2011.
[22] S. Kajita et al., J. Nucl. Mater. 418 (2011) 152.
[23] S.I. Krasheninnikov, Phys. Scr. T145 (2011) 014040.
[24] M.B. Toloczko, J.P. Hirth, F.A. Garner, J. Nucl. Mater. 283–287 (2000) 409.
[25] M.A. Meyers, K.K. Chawla, Mechanical Behavior of Materials, Cambridge University Press, 2009.
[26] K.O.E. Henriksson et al., Nucl. Instr. Meth. Phys. Res. B 244 (2006) 377.
[27] R.D. Smirnov, S.I. Krasheninnikov, J. Nucl. Mater., submitted for publication.
[28] S.J. Plimpton, J. Comput. Phys. 117 (1995) 1.
[29] http://www.ctcms.nist.gov/potentials/W.html.
[30] D.F. Bahr, D.E. Kramer, W.W. Gerberich, Acta Mater. 46 (1998) 3605.
[31] J.F. Ziegler, J.P. Biersack, U. Littmark, Stopping and Ranges of Ions in Matter, vol. 1, Pergamon Press, 1985.
[32] K.O.E. Henriksson et al., Phys. Scr. T108 (2004) 95.
[33] D.E. Beck, Mol. Phys. 14 (1968) 311, Mol. Phys. 15 (1968) 332.